Cyclostationary noise modeling of radio frequency devices

INTERNATIONAL JOURNAL OF NUMERICAL MODELLING: ELECTRONIC NETWORKS, DEVICES AND FIELDS
Int. J. Numer. Model. 2013; **00**:1–15
Published online in Wiley InterScience (www.interscience.wiley.com). DOI: 10.1002/jnm

Cyclostationary noise modeling of RF devices

F. Bonani[1]*, S. Donati Guerrieri[1], G. Ghione[1]

[1]*Dipartimento di Elettronica e Telecomunicazioni, Politecnico di Torino, Corso Duca degli Abruzzi 24, 10129 Torino, Italy*

SUMMARY

We present a review of the current status of research in the modeling and simulation of cyclostationary (nonlinear) noise properties of semiconductor active devices operated in forced large-signal conditions, a typical operating regime for high frequency applications. We discuss both the case of physics-based device simulations, where numerical burden is the most important issue, and the derivation of compact cyclostationary noise models. In the latter case, both phenomenological amplitude modulation approaches and the derivation of consistent analytical device descriptions are discussed. We show examples of both physics-based simulations of the noise properties of a realistic HEMT resistive mixer, and show for the first time the application of a novel, fully analytical cyclostationary noise bipolar transistor model. Copyright © 2013 John Wiley & Sons, Ltd.

Received ...

KEY WORDS: semiconductor device modeling, semiconductor device noise, cyclostationary noise

1. INTRODUCTION

Noise arising in active semiconductor devices often poses the ultimate limit to the optimization of circuit performances, like in the development of modern communication systems or accurate instrumentation equipment. In many fields, including wireless communications and remote sensing, the operating frequency is constantly increasing, thus calling for accurate active device noise models in the RF and microwave frequency range. Furthermore, in many subsystems where noise is a main concern, such as the receiver chain of a RX-TX module, the nonlinear (e.g. mixers) or linear blocks (e.g. Low Noise Amplifiers, LNAs) may be subject to saturation due to strong input or interfering signals. In this case the device operating condition already in the ideal noiseless case is time-varying and highly nonlinear in response to the external inputs. Concerning noise analysis, the computer aided design and optimization of such subsystems requires the development of the so called *cyclostationary noise models*, i.e. noise models that can predict the noise device behavior when its operating condition is nonstationary, and in particular periodically time-varying (Large Signal – LS – operation) [1–3]. Under this respect, cyclostationary noise is often referred to as *nonlinear device noise*.

The cyclostationary noise analysis is by far more involved than the stationary one, where the device operating point is instead time-independent (sometimes referred to as linear or small-signal noise). In fact, in the nonlinear case noise measurement capabilities are limited and, contrary to the stationary (linear, small-signal) case, they cannot provide a full characterization of the terminal device noise performances (see [4] and references therein). Since a complete and easily available noise characterization is lacking, the development of accurate nonlinear noise models is essential.

*Correspondence to: E-mail: fabrizio.bonani@polito.it

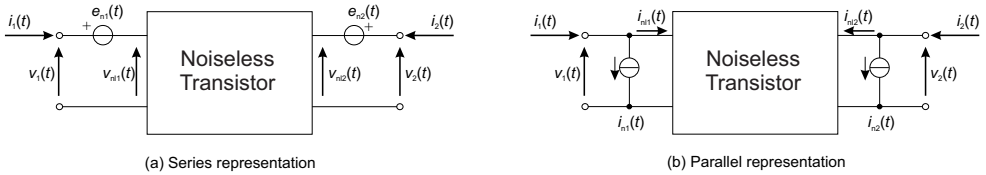

Figure 1. (a) Series and (b) parallel circuit representation of a noisy transistor in time domain. The subscript "nl" indicates noiseless quantities

However, even in this case various issues arise that ultimately limit the ease of identification of a seamless model, where the device noise properties are included in a self-consistent way with all the other device electrical performances in LS operating conditions. While compact models have been proposed, where simplified approximate cyclostationary noise is included in a non fully self-consistent way, the remarkable numerical effort required for physics-based device simulation in nonlinear conditions has hindered the development of cyclostationary noise analysis until recent years [3].

This paper aims at reviewing viable approaches to the cyclostationary noise analysis of semiconductor devices. Particular emphasis is posed on the approximations that can be made, leading to a full set of cyclostationary noise models, that range from the more accurate to the simpler, albeit approximate, approaches. Starting from the description of microscopic fluctuations in the nonlinear case, the accurate physics-based nonlinear noise analysis is presented, with particular emphasis on the so called Conversion Green's Function (CGF) approach [2, 3, 5]. Also, compact models are discussed in detail, showing that, while approximate solutions may be exploited in the development of a nonlinear noise model starting from the linear (stationary) case, accurate compact models can also be derived in a rigorous way.

Although a great variety of examples of ciclostationary noise analysis could be provided, in this paper we have focused the attention on two particular case studies. The examples presented show that the accurate nonlinear noise analysis of RF semiconductor devices is actually feasible both at the physics-based and at the compact model level, providing a solid link between the device physical properties and structure and the final circuit noise performances. The examples discussed include a microwave field-effect transistor (a GaAs HEMT) and a Si bipolar transistor (BJT). In the latter case, a novel and fully consistent compact model for bipolar transistors including cyclostationary noise in a seamless way within the LS device model is presented. To the author's knowledge, this is the first nonlinear BJT model embedding noise analysis presented in the literature. Although the model is limited, in its present formulation, to homostructure BJTs, the extension to the heterostrutcure bipolar transistor (HBT) case, more interesting for the microwave and millimeter wave frequency range, is also feasible.

2. CIRCUIT REPRESENTATION OF NOISY TRANSISTORS

The circuit representation of noisy devices is based on the assumption that, since fluctuations induce a small perturbation of the noiseless device steady-state, they can be interpeted as small-amplitude, zero average random signals superimposed to the (noiseless) currents and voltages at the device ports (see e.g., [5]). From a circuit viewepoint, this statement is equivalent to introducing impressed random (zero average) *noise generators* at the device ports. In the present discussion we consider as a modeling case study the transistor, i.e. a two-port device. Accordingly, we may have input and output voltage or current noise generators, in any possible combination. For the sake of simplicity, we only show in Fig. 1 the series and parallel equivalent circuits.

Denoting the vector quantities (currents $\mathbf{i}$ and voltages $\mathbf{v}$) obtained collecting the elements pertaining to port 1 and 2, respectively, we have:

$$\mathbf{v}(t) = \mathbf{v}_{\rm nl}(t) + \mathbf{e}_{\rm n}(t) \qquad \text{series representation} \tag{1}$$

DOI: 10.1002/jnm

$$\mathbf{i}(t) = \mathbf{i}_{\mathrm{nl}}(t) + \mathbf{i}_{\mathrm{n}}(t) \qquad \text{parallel representation} \tag{2}$$

where subscript "nl" indicates noiseless quantities. The noise generators are usually assumed gaussian random processes, and therefore are fully characterized by their second order moments (being the average equal to zero). The relevant quantity is therefore the correlation matrix (hereafter presented in terms of current generators only):

$$\mathbf{R}_{\mathbf{i}_{\mathrm{n}},\mathbf{i}_{\mathrm{n}}}(t_1,t_2) = \left\langle \mathbf{i}_{\mathrm{n}}(t_1)\mathbf{i}_{\mathrm{n}}^{\mathrm{T}}(t_2)\right\rangle \tag{3}$$

where $\langle\cdot\rangle$ is the statistical average, and $^{\mathrm{T}}$ denotes the transpose. The elements of $\mathbf{R}$ are the correlation functions of the respective elements of the random generator vectors.

The statistical properties of the generators have a deep impact on the correlation matrix, and in turn depend on the transistor operating conditions [3,5]: in the simplest case, the noiseless operating point is DC. This condition is typical, e.g., of low-noise amplifiers (LNAs), and implies that the stochastic processes representing noise are *stationary*:

$$\mathbf{R}_{\mathbf{i}_{\mathrm{n}},\mathbf{i}_{\mathrm{n}}}(t_1,t_2) = \mathbf{R}_{\mathbf{i}_{\mathrm{n}},\mathbf{i}_{\mathrm{n}}}(t_2-t_1). \tag{4}$$

As a consequence, an equivalent representation in the frequency domain is provided by the *noise spectrum*, i.e. the Fourier transform of the correlation matrix:

$$\mathbf{S}_{\mathbf{i}_{\mathrm{n}},\mathbf{i}_{\mathrm{n}}}(\omega) = \mathcal{F}\left\{\mathbf{R}_{\mathbf{i}_{\mathrm{n}},\mathbf{i}_{\mathrm{n}}}(\tau)\right\}. \tag{5}$$

Noise spectra can be experimentally derived from direct measurements; however, in high-frequency devices, system oriented noise parameters (such as the noise figure, the noise resistance and the optimum noise input impedance) are usually derived from the experiment [6]. Starting from these and from the measured small-signal (e.g. scattering) parameters, straightforward analytical manipulations allow to derive the noise spectra. The opposite path is of course followed when the noise spectra are obtained from modeling approaches and the system oriented noise parameters are then derived therefrom [5].

A more complex case is that of devices driven into *periodic* (or *quasi-periodic*) operating conditions, also denoted as Large-Signal (LS) operation. Important examples of this operating regime are mixers, frequency multipliers and power amplifiers (although in the latter case noise is rarely an important issue). In LS, the noiseless working point is strictly periodic or a superposition of non-commensurate sinusoidal tones, in the quasi-periodic case: for the sake of simplicity we discuss here the strictly periodic case, the extension being trivial. Therefore the time-varying working point amplitude modulates the noise processes taking place in the device (see Section 3). The consequence of the modulation is a profound change in the statistical features of fluctuations [2,5,7,8]: the random processes are no longer stationary, but rather *cyclostationary*.

Cyclostationary processes are characterized, in time domain, by a correlation matrix that is doubly periodic of the same period T of the LS working point. In the frequency domain, this periodicity constraint amounts to the following: the frequency axis is divided into frequency ranges, called *sidebands,* that define a neighborhood of each harmonic of the fundamental (angular) frequency $\omega_{\mathrm{f}} = 1/T$. We have the k-th (k is integer) *upper sideband* $\omega_k^+ = k\omega_{\mathrm{f}} + \omega$ and the *lower sideband* $\omega_k^- = k\omega_{\mathrm{f}} - \omega$, where $0 \le \omega \le \omega_{\mathrm{f}}/2$ is the *sideband (angular) frequency*. The main feature of cyclostationary processes is that their frequency components are correlated (as for nonstationary processes) if and only if we consider frequencies whose distance from one of the LS harmonics is the same, i.e. correlation takes place only between sidebands, see Fig. 2 for a graphical representation of the cyclostationary process correlation spectrum.

As a consequence, the frequency domain characterization of the cyclostationary noise is provided by the *sideband correlation matrix* (SCM), the collection of all the possible correlation spectra between all the possible sidebands for each of the involved noise processes. Using only the *upper* sideband SCM (see again Fig. 2) is sufficient to fully characterize the noise, since a double sided spectrum is used and the correlation spectra turn out to be symmetric with respect to the zero absolute frequency because noise processes are real-valued in the time domain [3]. Notice, though,

DOI: 10.1002/jnm

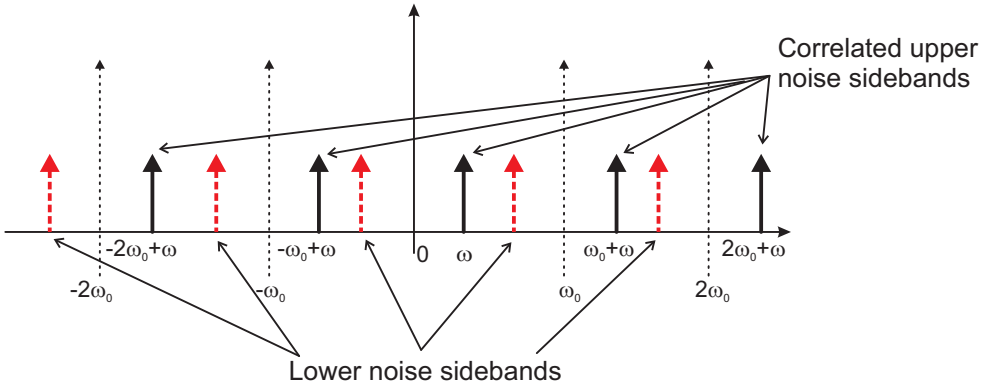

Figure 2. Noise sidebands and their correlation. In principle, all the noise sidebands are correlated. However, since the fluctuations are real signals, the correlation among the upper sidebands only is sufficient to fully represent the second order statistical properties. Correlation depends only on the sideband frequency ω.

that only the diagonal elements of the SCM can be actually measured. For instance, the element $(1,1)$, the self-correlation of the upper sideband on the right of the LS fundamental, is the *residual phase noise* [4].

From the numerical standpoint, any evaluation of the cyclostationary noise requires two steps: first the periodic noiseless steady state must be evaluated. In this step the spectrum must be truncated to some harmonic order N_S and each variable describing the noiseless device working point (voltage, current or any internal physical quantity like the carrier number) will require $(2N_S + 1)$ real numbers (namely N_S conjugate complex numers + DC) for a full mathematical description. In the second step we turn to the evaluation of the sideband correlation matrix representing noise: here we will have one upper sideband for each of the harmonics of the steady state, hence the noise generator is represented by a SCM of $(2N_S + 1) \times (2N_S + 1)$ complex numbers (see e.g. [3] for details).

A different treatment is required for the noise analysis of autonomous systems, namely oscillators, where the lack of a specified time reference induced by the forcing generators implies a much more complex behaviour. Recent results indicate that the asymptotic behaviour of fluctuations turns back to stationary noise processes, despite in oscillators the working point is clearly LS [9–11]. From the device modeling standpoint, therefore, the stationary noise generator spectra are the pre-requisite for a complete oscillator noise analysis.

3. AMPLITUDE MODULATION OF STATIONARY FLUCTUATIONS

As discussed above, amplitude modulation is the key process leading to cyclostationary noise. From a physical standpoint, the modulation is provided by the fact that in the vast majority of cases stationary fluctuations are represented by random processes whose amplitude depends on quantities that, in turn, are an expression of the noiseless device working point. Notice that this is valid both at the compact modeling level and at the microscopic level. At the compact model level, think e.g. of the shot noise associated to the collector noise current generator of a bipolar transistor (being it homo- or hetero-junction): $S_{i_C,i_C} = 2qI_C$ where q is the (absolute value of the) electron charge and I_C is the collector current in the DC bias point. At the microscopic level, typical examples are the fundamental fluctuations of the charged carrier number (generation-recombination – GR – noise) or carrier velocity (diffusion noise) which depend, in turn, on the microscopic noiseless steady state. Notice that microscopic noise processes are often interpreted as the microscopic noise sources [5], meaning that noise at the microscopic level will be the source for the induced noise at the external device terminals: such transfer from the microscopic to the macroscopic (external) noise is also the basis of the Green's Function Method which will be described more in detail in the following Sec. 4.1 (see also Fig.4 (a) below).

DOI: 10.1002/jnm

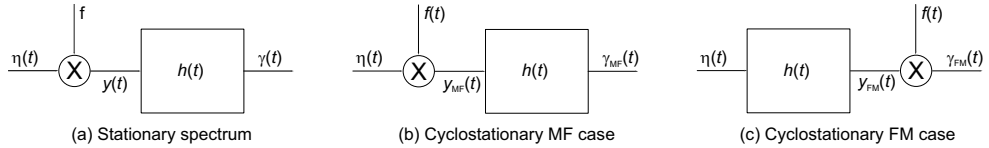

Figure 3. Possible system representations of amplitude modulation. (a) Stationary spectrum. (b) LS MF case. (c) LS FM case.

While microscopic fluctuations may seem to be a more fundamental description of the device noise, from the modelling standpoint it is worth to keep the treatment general, so that here we shall merely assume that all the stationary noise processes (microscopic or measured at the device terminals) are described as a function of the noiseless steady state of the system.

Obviously, when the noiseless working point becomes time-varying, amplitude modulation occurs and the previous description of noise through stationary processes needs to be revisited in terms of cyclostatonary processes. The extraction of the cyclostationary process arising from amplitude modulation is not at all a trivial issue. In particular, we will show that the modulation procedure is uniquely defined only for a white stationary process, whereas in the case of colored processes only approximations can be made.

The issue of colored noise is not at all trivial. In fact, while some examples of white stationary noise are known (like e.g. the above mentioned shot noise and GR and diffusion microscopic noise), in many cases stationary fluctuations are characterized by colored spectra. This may be due to fundamental considerations, as for the fluctuations associated to low-frequency noise [4]. However, in many compact models colored fluctuation spectra simply derive from reactive effects in the device, that filter the possibly white noise generators: consider e.g. the series noise representation of a bipolar transistor, where noise generators have colored spectra, as opposed to the parallel representation, where generators (at least, neglecting GR noise) are white.

In order to highlight the modulation issues, let us consider a scalar stationary random process $\gamma(t)$ (the case of vector random processes can be treated similarly) characterized by the spectrum $S_{\gamma,\gamma}(\omega)$. In semiconductor devices, $\gamma(t)$ can be practically always expressed according to the system interpretation in Fig. 3 (a) [3, 7, 8], where $\eta(t)$ is a gaussian, unit white noise random process, factor f depends on the DC working point and $h(t)$ is the impulse response of a linear time invariant (LTI) system that provides the coloring to the noise spectrum (filtering block):

$$S_{\gamma,\gamma}(\omega) = f^2 \left|\tilde{h}(\omega)\right|^2, \tag{6}$$

$\tilde{h}(\omega)$ being the Fourier transform of $h(t)$. Clearly, the case of white noise is characterized by $\tilde{h}(\omega) = 1$. From a modeling standpoint, the identification of f and $\tilde{h}(\omega)$ from (6) is of course not unique, thus calling for the availablity of either measurements or physics-based simulations (even of idealized structures) to uniquely identify the model.

Turning to LS operation, function f becomes periodically time-varying as a function of the LS working point, and the amplitude modulation takes place. The main difficulty is that such a modulation is not uniquely defined, being possible at least the two choices sketched in Fig. 3 (b) and (c):

1. modulation followed by filtering (MF, Fig. 3 (b)), for which the element (m, n) of the SCM for the MF modulated process reads:
$$\left(\mathbf{S}_{\gamma_{\mathrm{MF}},\gamma_{\mathrm{MF}}}(\omega)\right)_{m,n} = \tilde{h}(\omega_m^+)\tilde{g}_{m-n}\tilde{h}^*(\omega_n^+) \tag{7}$$
where $\tilde{g}_k$ is the k-th harmonic component (coefficient of the exponential Fourier series) of the T-periodic function $g(t) = f^2(t)$, and * denotes the complex conjugate;
2. filtering followed by modulation (FM, Fig. 3 (c)), leading to the SCM for the FM modulated process:
$$\left(\mathbf{S}_{\gamma_{\mathrm{FM}},\gamma_{\mathrm{FM}}}(\omega)\right)_{m,n} = \sum_k \tilde{f}_{m-k}\tilde{f}^*_{n-k}\left|\tilde{h}(\omega_k^+)\right|^2. \tag{8}$$

DOI: 10.1002/jnm

The two approaches lead to the same result for white stationary processes ($\tilde{h}(\omega) = 1$):

$$(\mathbf{S}_{\gamma_{\mathrm{MF}},\gamma_{\mathrm{MF}}})_{m,n} = \tilde{g}_{m-n} = \sum_k \tilde{f}_{m-k}\tilde{f}^*_{n-k} = (\mathbf{S}_{\gamma_{\mathrm{MF}},\gamma_{\mathrm{MF}}})_{m,n}\,, \tag{9}$$

as follows from the properties of the Fourier series of $g(t) = f^2(t)$. On the other hand, the case of colored noise yields markedly different behaviours. Let us consider the common (but not unique) case of a low-pass stationary frequency behaviour characterized by a corner frequency $\omega_{\mathrm{c}} \ll \omega_{\mathrm{f}}$ (a typical condition of low-frequency noise [4]), thus implying that $\tilde{h}(\omega) \approx 0$ if $\omega_{\mathrm{c}} \ll \omega \ll \omega_{\mathrm{f}}/2$ or, in other words, $\tilde{h}(\omega_k^+) \approx 0\ \forall k \neq 0$. Equation (7) yields

$$(\mathbf{S}_{\gamma_{\mathrm{MF}},\gamma_{\mathrm{MF}}}(\omega))_{m,n} = \begin{cases} \tilde{h}(\omega_0^+)\tilde{g}_0\tilde{h}^*(\omega_0^+) & \text{for } m = n = 0 \\ 0 & \text{in all other cases} \end{cases}, \tag{10}$$

while in (8)

$$(\mathbf{S}_{\gamma_{\mathrm{FM}},\gamma_{\mathrm{FM}}}(\omega))_{m,n} \approx \tilde{f}_m\tilde{f}^*_n\left|\tilde{h}(\omega_0^+)\right|^2 \qquad \forall m, n. \tag{11}$$

These results mean that the MF modulation does not provide any frequency conversion, the only element of the modulated process SCM different from zero being the baseband sideband, while FM guarantees the upconversion of low frequency noise components up to all the available sidebands, provided that the modulating function $f(t)$ is endowed with large enough harmonic components.

Notice that none of the two possible modulation choices discussed here may be the exact one, unless the stationary process is white. A comparison with experimental results is therefore unavoidable to assess the model accuracy. In some cases, however, a clue on possibly articulated modulation strategies may be suggested by physics-based noise simulations (see e.g. Section 4.2 below).

4. CYCLOSTATIONARY NOISE MODELING

The structural and parametric identification of device cyclostationary noise models ultimately aims at finding the SCM of the device terminal noise generators, being the latter current (parallel representation) or voltage (series representation) as a function of the LS working point. Notice that all representations are equivalent and even more complex schemes can be developed, e.g. with all the noise sources placed at the input port, akin to the representation of noise based on noise figure and optimum noise resistance often used at the circuit level in the stationary case. Since comparatively simple linear transformations, involving the device conversion matrix, can be exploited to transform from one noise representation to the other [3, 5], in this work we focus our attention on the description of the device level parallel noise models.

4.1. Physics-based models

The physical simulation of semiconductor devices is based on the solution of a microscopic physical model that describes the dynamics of the charged carriers, ultimately providing the device current flow as a function of the electrical generators applied to the device terminals. Several levels of physics-based (PB) models exhist, characterized by the complexity of the description of carrier dynamics, from semi-classical to quantum [12].

Focusing on device noise simulation, PB noise analysis aims at finding the second-order statistical properties of the terminal noise generators as a function of the device working point [3]. In the case of cyclostationary noise analysis, this amounts to estimate the noise generators' SCM.

Currently, PB cyclostationary noise analysis has been implemented for semiclassical carrier transport only, i.e. no quantum transport simulations are yet available. Even within this case, many options are potentially available: either the full Boltzmann Transport Equation (BTE) [12] is exploited to describe carrier transport, or the approach may be based on suitable moments of the

DOI: 10.1002/jnm

BTE leading to partial-differential equation (PDE) based models. Among these the drift-diffusion, energy-balance and full hydrodynamic descriptions are the most popular.

The solution of the BTE can be carried out in two ways. The most popular is a time-domain per-particle integration introducing a randomization, i.e. the Monte Carlo method (see e.g. [13]). In this approach, fluctuations are embedded in the numerical solution technique, and therefore the estimation of the SCM can be performed directly from the time-series resulting from the repeated solutions of the BTE. Being a time-domain method, this approach makes it very hard the study of cyclostationary noise properties at comparatively low frequency, because the time-frequency transformations require very long integration times. Nevertheless, this approach has been succesfully exploited by some research groups [14–17].

A different, deterministic approach to BTE solution (including noise) was proposed in [18, 19]. In this case, the BTE is projected onto spherical harmonics in the momentum space, thus leading to a set of time- and space-dependent PDEs. This approach has the advantage of admitting the use of both time- and frequency-domain approaches (after spatial discretization) for the solution of the BTE, and ultimately all the numerical techniques developed for PDE PB models for noise analysis [3]. However, the introduction of fluctuations in this modeling approach requires the explicit insertion of stochastic forcing terms in the right-hand-side (r.h.s.) of the BTE, represented by zero average random processes that describe the occurrence of carrier velocity and number fluctuations taking place at the microscopic level (see [18, 19] for details). For this reason, these are called *microscopic noise sources* of the model.

The concept of microscopic noise source is the core of noise analysis even for the much more common PDE PB noise models. Although microscopic noise sources can be devised for non-stationary transport models defining them as the moments of the BTE microscopic noise sources [20, 21], in many cases the simpler drift-diffusion (DD) transport model is used. In this case, theoretical considerations allow to analytically express the stationary microscopic noise sources for the two most important causes of fluctuations in semiconductors [3, 5] in terms of white noise processes:

- fluctuations in the *velocity* of the charged carriers, that in case of the DD PB model induce current density fluctuations proportional to the carrier concentration times the noise diffusion coefficient. This noise source is also called *diffusion noise*;
- fluctuations in the *number* of charged carriers, whose spectrum is proportional to the sum of the generation rate and of the recombination rate. This leads to the *generation-recombination (GR) noise* source.

A third microscopic noise source is provided for the $1/f$ or *flicker noise*. Since the very physical origin of this is still a matter of debate, a phenomenological stationary microscopic noise source embedding already a $1/f$ frequency behaviour is often used [3, 5].

Turning to the LS case, the above stationary microscopic noise sources must be converted into cyclostationary ones through amplitude modulation. The key difference is played by the use of white (GR o diffusion noise) or colored (*flicker noise*) stationary microscopic noise sources, because only in the first case the amplitude modulation induced by the LS working point leads to uniquely defined cyclostationary microscopic noise sources (see the discussion in Section 3).

A very effective technique for PDE PB noise analysis is through the so-called Green's Function (GF) approach. Such a method is essentially a generalization of the classical Shockley's Impedance Field [22]. Due to its ease of use, compatibility with standard PDE-based numerical device simulators and numerical efficiency, the GF method is the most widespread device level noise analysis technique, at least at the stationary level, also because its generalization to the nonlinear case has been demonstrated. Here we will highlight the most important features of the GF approach in the LS case, which is also the basis of the examples shown in the following sections. Let us assume that the microscopic noise source introduced in equation α of the PDE system is denoted as $\gamma_\alpha(\mathbf{r}, t)$: in the conventional Drift-Diffusion model $\alpha = n, p$ stands for the continuity equation of electrons and hole, respectively. The basic assumption of noise analysis in forced device operation (both stationary and cyclostationary) is the small-change approximation based on the small amplitude

DOI: 10.1002/jnm

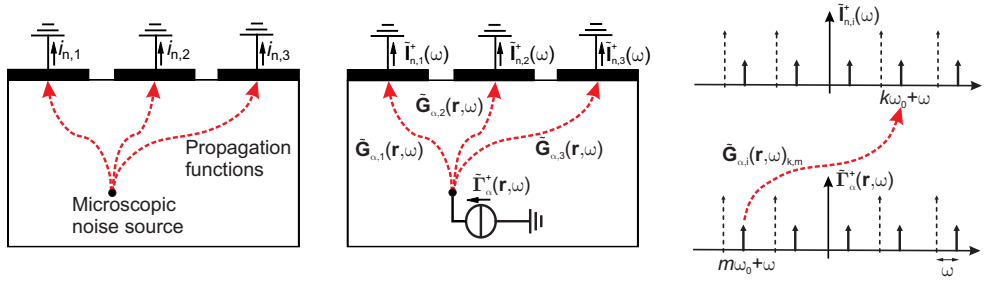

Figure 4. Graphical representation of the Green's Function Method for a 3-terminal device: (a) in each internal point a microscopic noise source induces a short-circuit noise current at each device terminal. (b) Microscopic noise is represented by an equivalent current source $\tilde{\mathbf{\Gamma}}^{+}_{\alpha}(\mathbf{r},\omega)$, collecting all the sidebands. The Conversion Green's Function $\tilde{\mathbf{G}}_{\alpha,i}(\mathbf{r},\omega)$ converts the microscopic noise into the $i-$th terminal noise sidebands $\tilde{\mathbf{I}}^{+}_{\mathrm{n},i}$ $(i=1,2,3)$. (c) Source and terminal noise spectra showing the CGF element converting the microscopic m-th sideband component to the k-th sideband terminal noise. In the example: $m=-2$, $k=1$.

of the microscopic noise sources, that allows for a linear approximation of the propagation of the microscopic fluctuations to the device terminals (see Fig.4 (a)).

This makes it possible to define the propagation by means of a Green's function $G_{\alpha,i}(\mathbf{r};t,t_1)$ where i denotes the observation terminal, $\mathbf{r}$ the injection point, t the observation instant and t_1 the injection instant. Two types of Green's functions can be defined, according to the type of terminal noise generators: short circuit current or open-circuit voltage, respectively used to calculate the current or voltage noise generators [3,5,23]. For the current noise generators, for each terminal i we find

$$i_{\mathrm{n},i}(t)=\sum_{\alpha}\int_{\Omega}\int_{-\infty}^{t}G_{\alpha,i}(\mathbf{r};t,t_1)\gamma_{\alpha}(\mathbf{r};t_1)\,\mathrm{d}t_1\mathrm{d}\mathbf{r}, \tag{12}$$

where Ω is the device volume. While for stationary noise analysis $G_{\alpha,i}(\mathbf{r};t,t_1)=G_{\alpha,i}(\mathbf{r};t-t_1)$, i.e. the linear transformation is time-invariant, thus allowing for an efficient treatment of the time integral in (12) in the frequency domain, the case of cyclostationary fluctuations is more involved.

Due to the time-periodic nature of the noiseless working point, the linearized system becomes periodically time-varying [2, 3] causing two main effects: the microscopic noise sources undergo frequency conversion among the various sidebands, and the Green's functions become, in the frequency domain, spatially dependent *Conversion Green's Functions* (CGFs). The details of this treatment can be found in [2]; we summarize here the results. Let us collect the $2N_{\mathrm{S}}+1$ amplitudes of the upper sidebands of the noise generator into a vector denoted as $\tilde{\mathbf{I}}^{+}_{\mathrm{n},i}$, and those of the microscopic noise sources into $\tilde{\mathbf{\Gamma}}^{+}_{\alpha}(\mathbf{r})$. Equation (12) becomes

$$\tilde{\mathbf{I}}^{+}_{\mathrm{n},i}=\sum_{\alpha}\int_{\Omega}\tilde{\mathbf{G}}_{\alpha,i}(\mathbf{r},\omega)\tilde{\mathbf{\Gamma}}^{+}_{\alpha}(\mathbf{r})\,\mathrm{d}\mathbf{r}, \tag{13}$$

where $\tilde{\mathbf{G}}_{\alpha,i}(\mathbf{r},\omega)$ is the $(2N_{\mathrm{S}}+1)\times(2N_{\mathrm{S}}+1)$ CGF. A graphical representation of (13) is skeched in fig. 4 (b) and the detailed explanation of the frequency conversion among sidebands from the microscopic to the device terminal can be found in Fig 4 (c). The SCM of the noise generators connected to terminal i and j is then easily derived from (13)

$$\mathbf{S}_{i_{\mathrm{n},i},i_{\mathrm{n},j}}(\omega)=\sum_{\alpha,\beta}\int_{\Omega}\tilde{\mathbf{G}}_{\alpha,i}(\mathbf{r},\omega)\tilde{\mathbf{K}}_{\gamma_\alpha,\gamma_\beta}(\mathbf{r},\omega)\tilde{\mathbf{G}}^{\dagger}_{\beta,j}(\mathbf{r},\omega)\,\mathrm{d}\mathbf{r}, \tag{14}$$

where † denotes the hermitian conjugate, and we have made the customary assumption of spatially uncorrelated microscopic noise sources, i.e.

$$\mathbf{S}_{\gamma_\alpha,\gamma_\beta}(\omega)=\left\langle\tilde{\mathbf{\Gamma}}^{+}_{\alpha}(\mathbf{r}_1)\tilde{\mathbf{\Gamma}}^{+\dagger}_{\beta}(\mathbf{r}_2)\right\rangle=\tilde{\mathbf{K}}_{\gamma_\alpha,\gamma_\beta}(\mathbf{r}_1,\omega)\delta(\mathbf{r}_1-\mathbf{r}_2). \tag{15}$$

DOI: 10.1002/jnm

Clearly, from the modeling standpoint the computationally intensive task is the determination of the CGFs. In fact, in principle for each equation and terminal, and for each couple of sideband indices, $\mathbf{G}_{\alpha,i}$ should be computed by injecting a unit, impulsive source (a delta function) in each of the spatial discretization nodes, thus requiring a very large number of solutions of the linearized device model. To be more precise, if N_{eq} is the number of equations in the PDE system, N_{t} the number of device terminal minus one, and N_{p} the number of mesh points, the order of magnitude of the required direct solutions would be, for each couple of sideband indices, $N_{\mathrm{eq}}N_{\mathrm{t}}N_{\mathrm{p}}$.

This number can be dramatically decreased to N_{t}, for each couple of sideband indices, exploiting the generalized adjoint approach discussed in [2], a generalization to LS operation of the original adjoint approach introduced for stationary noise analysis in [23].

To the best of our knowledge, cyclostationary noise analysis has not been yet implemented into commercial CAD tools for device PB modeling: academic implementations only [2, 24–28] are currently available. On the other hand, stationary PB noise analysis is currently available in all the major tools exploiting an implementation of the adjoint method [23].

4.2. Compact models

Compact cyclostationary noise models are analytical or numerical models where the SCM of the device noise generators is evaluated as a function of the noiseless device LS working point. As such, they play a fundamental role in the design and optimization of low noise nonlinear systems, since the compact model can be used in circuit simulators in order to allow for the circuit design.

Such models are usually derived in two possible ways. The first is to derive the compact noise model starting from a PB noise model (almost always based on the DD description of carrier transport), complemented by a suitable set of simplifying assumptions in order to make the PB model analytically treatable. In practice, this amounts to simplify the PB model in order to make the analytical evaluation of the CGFs feasible. Examples of this strategy are the analytical compact model for pn junctions presented in [29, 30], based on a generalization to the LS operation of the classical Shockley model for pn junctions, or the compact modeling strategy for the simulation of cyclostationary low-frequency (random telegraph signal – RTS) noise in MOSFETs [31].

The second approach, by far the most easily found in the literature, is based on the amplitude modulation of a previously assessed stationary noise compact model, along the lines of the discussion in Section 3. According to a survey of the literature, the FM approach is probably the most commonly applied in circuit simulators [32–34], although the MF approach has been exploited as well, at least for flicker noise [35, 36]. The FM modulation scheme corresponds to the cyclostationary sources discussed in [4], while the low-pass sources refer to MF modulation.

Clearly, the two modulation schemes are phenomenological interpretations of complex physical phenomena, that, moreover, are applied to terminal-level stationary compact models being already the result of important simplifying assumptions. Therefore, there is no a priori reason for either of the two providing an exact result, at least when colored noise generators are modulated. This statement is confirmed by several examples in the literature: the GR noise in a uniformly doped sample (a linear resistor) was studied in [8] showing that the FM approach yields exact results, while MF modulation applied to the classical van Vliet model [37] was shown in [3] to better approximate the current noise SCM of a pn junction, at least for the diagonal elements. This result was proved to be analytically exact in [30], where however it was also demonstrated that the off-diagonal SCM terms are not correctly reproduced by either modulation scheme.

Finally, the simulation of trap-assisted GR noise in a 2D pn junction demonstrated (see [4] and references therein) that if the microscopic noise sources act from very different regions of the device (in this case, traps located in the strongly nonlinear depletion layer, or the mostly linear neutral surface of the device), they may induce in the terminal SCM noise contributions that are following both possible modulation schemes: the FM approach for those sources that undergo frequency conversion (those in the depletion layer), and MF modulation for those that are not converted. This constitutes the physical basis for the complex modulation strategies that have been applied in [4, 38–40] to the cyclostationry noise simulation of heterostructure bipolar transistors validated by experimental results.

DOI: 10.1002/jnm

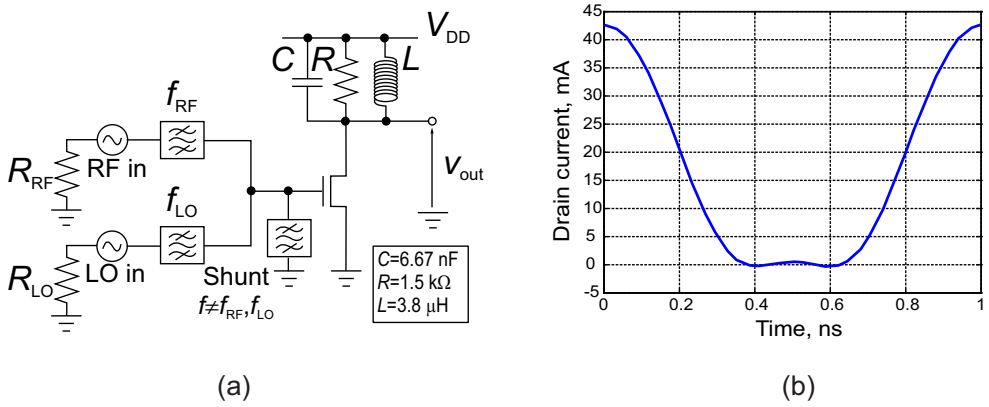

Figure 5. PB simulation of cyclostationary noise in a resistive HEMT mixer. (a) Scheme of the resistive mixer. (b) Time-dependence of the simulated HEMT drain current.

5. EXAMPLES

In order to provide a scenario of the capabilities and the relavance of the cyclostationary noise analysis, we will provide two examples, both of importance for high frequency devices, but different concerning the application standpoint. In a first example PB analysis is used *per se*, and the aim is to show the capability of the physics-based simulation to provide direct information on circuit design performances (a mixer case), starting from a very accurate description of the device physics. A second example is on the contrary oriented to modelling purposes. Here the PB analysis is used to validate a novel compact LS model for bipolar transistors, including cyclostationary noise in a self-consistent way. This model, at this stage limited to homojunction transistors, can be extended to the heterostructure case, hence resulting very interesting for high frequency nonlinear applications.

5.1. PB cyclostationary noise modeling of a resistive HEMT mixer

We consider first an example of physical simulation of cyclostationary noise, with reference to the 2D simulation of a resistive mixer based on a 0.5 μm gate double heterostructure GaAs based HEMT. The conductive channel is intrinsic $Al_{0.30}Ga_{0.70}As$ and the gate width is 100 μm, while the GaAs supply layer is doped 5×10^{18} cm^{-3}. The device is simulated by means of a 2D monopolar DD model, and the simulation is carried out including the circuit elements shown in Fig. 5 (a), since for a LS simulation the computation of the device working point cannot be performed in the absence of the embedding circuit [2, 3]; in other words, a mixed-mode simulation is required. The mesh is made of 4000 nodes, and the device is biased in class B (i.e., at the threshold of -0.4 V) with an imput tone at 1 GHz of amplitude 0.4 V. The local oscillator ($f_{\rm LO} = 1$ GHz) is assumed noiseless, while the RF input is at $f_{\rm RF} = 1.001$ GHz. The output resonator selects the downconverted intermediate frequency (IF) of 1 MHz with a 16 kHz bandwidth. The LS simulation is performed with the harmonic balance approach, including 4 harmonics plus DC and yielding, as an example of result, the time-domain drain current waveform shown in Fig. 5 (b). The device, that is off for almost half of period, cleary operates, in the large-signal working point, in strong nonlinear conditions.

Results of the PB noise simulation are shown in Fig. 6. More details on the analysis can be found in [41], where a MESFET resistive mixer was considered. The $(0, 0)$ element of the open circuit noise voltage SCM measured on the mixer load is shown in Fig. 6 (a) as a function of the sideband frequency. The partial contribution to the total noise spectrum due to the device diffusion noise microscopic noise source and the thermal noise of the RF input generator internal resistance are also presented, pointing out that the device contribution is the dominant one. From the input thermal noise and the total noise power spectum on the load resistance, the noise figure can be then extracted. Fig. 6 (b) shows the noise figure as a function of the value of the RF input generator

DOI: 10.1002/jnm

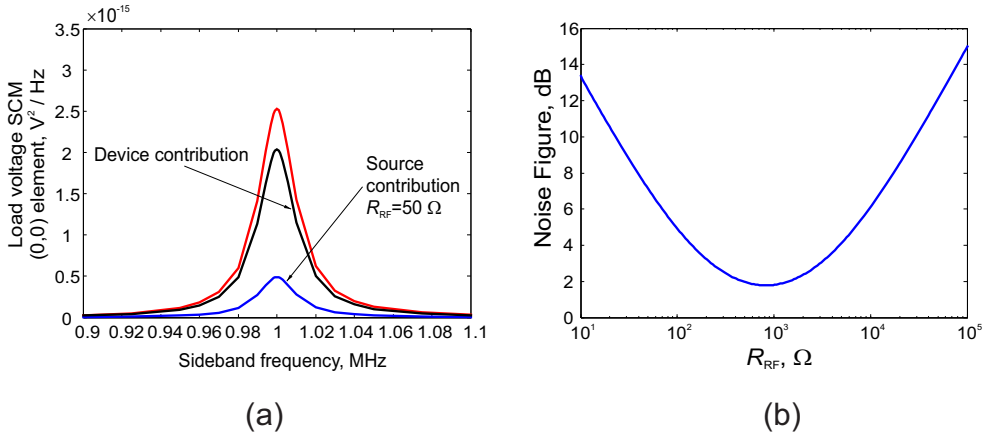

Figure 6. PB simulation of cyclostationary noise in a resistive HEMT mixer. (a) $(0,0)$ element of the open circuit voltage SCM calculated on the load. (b) Load noise figure as a function of the RF input resistance.

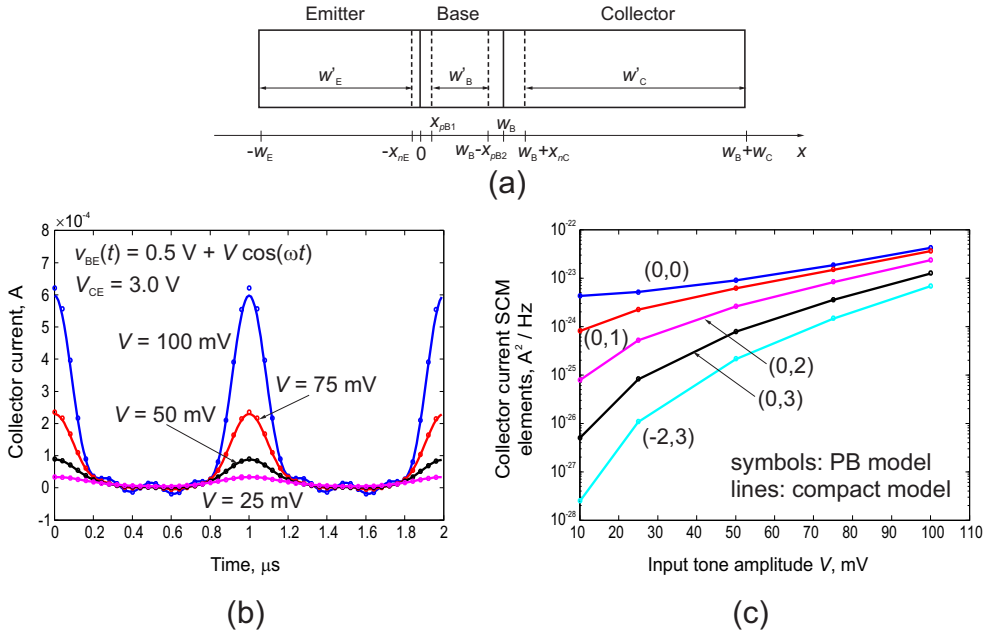

Figure 7. Compact model of cyclostationary noise in bipolar transistor. (a) Transistor simplified structure for the model derivation. (b) Time dependence of the collector current in LS operation. (c) Elements of the collector current noise SCM as a function of the input tone, after embedding of the parasitics.

resistance, thus demonstrating that the PB noise simulation can be exploited during the preliminary mixer design, since once R_{RF} is chosen a proper matching network can be easily designed.

5.2. Bipolar transistor cyclostationary noise compact model

We discuss here a novel, analytical cyclostationary noise compact model for bipolar transistors (BJTs) derived extending the treatment in [29]. The assumptions are the same as for the pn junction, and the model can be used to simulate, besides DC and small signal operation, also the LS performance of the device in terms of working point, conversion matrix and cyclostationary noise characteristics. The starting point is the simplified geometry shown in Fig. 7 (a) for a npn device. In a way similar to the pn junction case in [29], the drift-diffusion model is solved in the LS conditions, i.e. is converted into the frequency domain with periodic boundary conditions and analytically solved in one dimension within the quasi-neutral regions of the device. The resulting compact

Prepared using jnmauth.cls
DOI: 10.1002/jnm

model essentially extends the Ebers Moll model to the LS case. A linear expansion of the same model to the first order around the LS working point allows for the small-signal large-signal device analysis, hence extracting the device admittance correlation matrix. Finally the cyclostationary noise analysis is carried out by the analytical evaluation of the bipolar device CGFs and applying (14). The calculation of the LS working point and the admittance conversion matrix are not shown here for the sake of brevity while we outiline the main steps of the cyclostationary noise analysis.

As in the diode case, both GR and diffusion noise must be accounted for in the neutral regions of the device. The corresponding microscopic noise sources, i.e. the kernels of (14), are, in the LS case, described by their SCM: since the underlying noise processes are white, the amplitude modulation procedure is unique. Following (9), the elements of the source SCMs for diffusion and GR noise in the base region are:

$$\left(\tilde{\mathbf{K}}_{\mathbf{J}_\mathrm{B},\mathbf{J}_\mathrm{B}}(x)\right)_{k,m} = 4q^2 D_n \left[\tilde{n}'_{p,k-m}(x) + \frac{n_\mathrm{i}^2}{N_\mathrm{B}}\delta_{k,m}\right] \tag{16}$$

$$\left(\tilde{\mathbf{K}}_{\gamma_\mathrm{B},\gamma_\mathrm{B}}(x)\right)_{k,m} = \frac{2}{\tau_n}\left[\tilde{n}'_{p,k-m}(x) + \frac{n_\mathrm{i}^2}{N_\mathrm{B}}(1+\delta_{k,m})\right], \tag{17}$$

where $n'_p(x,t)$ the excess electron density and $\tilde{n}'_{p,i}(x)$ is the corresponding i-th harmonic component. Concerning physical parameters, n_i is the semiconductor intrinsic concentration, N_B the base doping, δ Kronecker symbol, D_n the electron noise diffusivity and τ_n the minority carrier lifetime in the base. Similar expressions hold for the emitter and collector neutral regions ($\alpha = \mathrm{E}, \mathrm{C}$):

$$\left(\tilde{\mathbf{K}}_{\mathbf{J}_\alpha,\mathbf{J}_\alpha}(x)\right)_{k,m} = 4q^2 D_{p\alpha}\left[\tilde{p}'_{n\alpha,k-m}(x) + \frac{n_\mathrm{i}^2}{N_\alpha}\delta_{k,m}\right] \tag{18}$$

$$\left(\tilde{\mathbf{K}}_{\gamma_\alpha,\gamma_\alpha}(x)\right)_{k,m} = \frac{2}{\tau_{p\alpha}}\left[\tilde{p}'_{n\alpha,k-m}(x) + \frac{n_\mathrm{i}^2}{N_\alpha}(1+\delta_{k,m})\right]. \tag{19}$$

There are four independent CGFs, corresponding to the effect on the emitter and collector current of the noise sources in the device neutral regions. Two Green's functions (Base-Emitter and Base-Collector) account for noise current in the emitter and collector terminals arising from the microscopic noise in the neutral base region, i.e.:

$$\left(\tilde{\mathbf{G}}_{I_\mathrm{E},\mathrm{B}}(x)\right)_{m,m} = -\frac{\sinh\left[\dfrac{x-(w_\mathrm{B}-x_{p\mathrm{B}2})}{\tilde{L}^+_{n,m}}\right]}{\sinh(\tilde{y}^+_{\mathrm{B},m})} \qquad \left(\tilde{\mathbf{G}}_{I_\mathrm{C},\mathrm{B}}(x)\right)_{m,m} = \frac{\sinh\left[\dfrac{x-x_{p\mathrm{B}1}}{\tilde{L}^+_{n,m}}\right]}{\sinh(\tilde{y}^+_{\mathrm{B},m})}, \tag{20}$$

where $x_{p\mathrm{B}1} \le x \le w_\mathrm{B} - x_{p\mathrm{B}2}$, $\tilde{L}^+_{n,m} = L_n/\sqrt{1+\mathrm{j}\omega^+_m\tau_n}$, $L_n = \sqrt{D_n\tau_n}$, and $\tilde{y}^+_{\mathrm{B},m} = (w'_\mathrm{B}/L_n)\sqrt{1+\mathrm{j}\omega^+_m\tau_n}$. Notice that the CGFs are diagonal, since the continuity equation for the excess minority carriers in the neutral region is linear (see [29]). Similarly, the effect on the emitter and collector current of the noise sources in the emitter and collector neutral region, respectively, is:

$$\left(\tilde{\mathbf{G}}_{I_\mathrm{E},\mathrm{E}}(x)\right)_{m,m} = \frac{\sinh\left[\dfrac{x+w_\mathrm{E}}{\tilde{L}^+_{p\mathrm{E},m}}\right]}{\sinh(\tilde{y}^+_{\mathrm{E},m})} \qquad \left(\tilde{\mathbf{G}}_{I_\mathrm{C},\mathrm{C}}(x)\right)_{m,m} = -\frac{\sinh\left[\dfrac{x-(w_\mathrm{B}+w_\mathrm{C})}{\tilde{L}^+_{p\mathrm{C},m}}\right]}{\sinh(\tilde{y}^+_{\mathrm{C},m})}, \tag{21}$$

where the two CGFs are defined for different ranges of x ($-w'_\mathrm{E} \le x \le -x_{n\mathrm{E}}$ the first, $w_\mathrm{B} + x_{n\mathrm{C}} \le x \le w_\mathrm{B} + w_\mathrm{C}$ the second), $\tilde{L}^+_{p\alpha,m} = L_{p\alpha}/\sqrt{1+\mathrm{j}\omega^+_m\tau_{p\alpha}}$, $L_{p\alpha} = \sqrt{D_{p\alpha}\tau_{p\alpha}}$, and $\tilde{y}^+_{\alpha,m} = (w'_\alpha/L_{p\alpha})\sqrt{1+\mathrm{j}\omega^+_m\tau_{p\alpha}}$ being $\alpha = \mathrm{E}, \mathrm{C}$.

DOI: 10.1002/jnm

Combining the microscopic noise sources and the CGFs, the SCM of the collector and emitter self and mutual correlation can be calculated as superposition integrals like in (14):

$$\left(\mathbf{S}_{i_{\mathrm{C}},i_{\mathrm{C}},\mathrm{Diff}}\right)_{k,m} = A\int_{x_{p\mathrm{B}1}}^{w_{\mathrm{B}}-x_{p\mathrm{B}2}} \frac{\partial\left(\tilde{\mathbf{G}}_{I_{\mathrm{C}},\mathrm{B}}\right)_{k,k}}{\partial x}\left(\tilde{\mathbf{K}}_{\mathbf{J}_{\mathrm{B}},\mathbf{J}_{\mathrm{B}}}\right)_{k,m}\frac{\partial\left(\tilde{\mathbf{G}}^{*}_{I_{\mathrm{C}},\mathrm{B}}\right)_{m,m}}{\partial x}\,\mathrm{d}x + A\int_{w_{\mathrm{B}}+x_{n\mathrm{C}}}^{w_{\mathrm{B}}+w_{\mathrm{C}}} \frac{\partial\left(\tilde{\mathbf{G}}_{I_{\mathrm{C}},\mathrm{C}}\right)_{k,k}}{\partial x}\left(\tilde{\mathbf{K}}_{\mathbf{J}_{\mathrm{C}},\mathbf{J}_{\mathrm{C}}}\right)_{k,m}\frac{\partial\left(\tilde{\mathbf{G}}^{*}_{I_{\mathrm{C}},\mathrm{C}}\right)_{m,m}}{\partial x}\,\mathrm{d}x \tag{22}$$

$$\left(\mathbf{S}_{i_{\mathrm{C}},i_{\mathrm{C}},\mathrm{GR}}\right)_{k,m} = q^2A\int_{x_{p\mathrm{B}1}}^{w_{\mathrm{B}}-x_{p\mathrm{B}2}} \left(\tilde{\mathbf{G}}_{I_{\mathrm{C}},\mathrm{B}}\right)_{k,k}\left(\tilde{\mathbf{K}}_{\gamma_{\mathrm{B}},\gamma_{\mathrm{B}}}\right)_{k,m}\left(\tilde{\mathbf{G}}^{*}_{I_{\mathrm{C}},\mathrm{B}}\right)_{m,m}\,\mathrm{d}x + q^2A\int_{w_{\mathrm{B}}+x_{n\mathrm{C}}}^{w_{\mathrm{B}}+w_{\mathrm{C}}} \left(\tilde{\mathbf{G}}_{I_{\mathrm{C}},\mathrm{C}}\right)_{k,k}\left(\tilde{\mathbf{K}}_{\gamma_{\mathrm{C}},\gamma_{\mathrm{C}}}\right)_{k,m}\left(\tilde{\mathbf{G}}^{*}_{I_{\mathrm{C}},\mathrm{C}}\right)_{m,m}\,\mathrm{d}x \tag{23}$$

$$\left(\mathbf{S}_{i_{\mathrm{E}},i_{\mathrm{E}},\mathrm{Diff}}\right)_{k,m} = A\int_{x_{p\mathrm{B}1}}^{w_{\mathrm{B}}-x_{p\mathrm{B}2}} \frac{\partial\left(\tilde{\mathbf{G}}_{I_{\mathrm{E}},\mathrm{B}}\right)_{k,k}}{\partial x}\left(\tilde{\mathbf{K}}_{\mathbf{J}_{\mathrm{B}},\mathbf{J}_{\mathrm{B}}}\right)_{k,m}\frac{\partial\left(\tilde{\mathbf{G}}^{*}_{I_{\mathrm{E}},\mathrm{B}}\right)_{m,m}}{\partial x}\,\mathrm{d}x + A\int_{-w_{\mathrm{E}}}^{-x_{n\mathrm{E}}} \frac{\partial\left(\tilde{\mathbf{G}}_{I_{\mathrm{E}},\mathrm{E}}\right)_{k,k}}{\partial x}\left(\tilde{\mathbf{K}}_{\mathbf{J}_{\mathrm{E}},\mathbf{J}_{\mathrm{E}}}\right)_{k,m}\frac{\partial\left(\tilde{\mathbf{G}}^{*}_{I_{\mathrm{E}},\mathrm{E}}\right)_{m,m}}{\partial x}\,\mathrm{d}x \tag{24}$$

$$\left(\mathbf{S}_{i_{\mathrm{E}},i_{\mathrm{E}},\mathrm{GR}}\right)_{k,m} = q^2A\int_{x_{p\mathrm{B}1}}^{w_{\mathrm{B}}-x_{p\mathrm{B}2}} \left(\tilde{\mathbf{G}}_{I_{\mathrm{E}},\mathrm{B}}\right)_{k,k}\left(\tilde{\mathbf{K}}_{\gamma_{\mathrm{B}},\gamma_{\mathrm{B}}}\right)_{k,m}\left(\tilde{\mathbf{G}}^{*}_{I_{\mathrm{E}},\mathrm{B}}\right)_{m,m}\,\mathrm{d}x + q^2A\int_{-w_{\mathrm{E}}}^{-x_{n\mathrm{E}}} \left(\tilde{\mathbf{G}}_{I_{\mathrm{E}},\mathrm{E}}\right)_{k,k}\left(\tilde{\mathbf{K}}_{\gamma_{\mathrm{E}},\gamma_{\mathrm{E}}}\right)_{k,m}\left(\tilde{\mathbf{G}}^{*}_{I_{\mathrm{E}},\mathrm{E}}\right)_{m,m}\,\mathrm{d}x \tag{25}$$

$$\left(\mathbf{S}_{i_{\mathrm{E}},i_{\mathrm{C}},\mathrm{Diff}}\right)_{k,m} = A\int_{x_{p\mathrm{B}1}}^{w_{\mathrm{B}}-x_{p\mathrm{B}2}} \frac{\partial\left(\tilde{\mathbf{G}}_{I_{\mathrm{E}},\mathrm{B}}\right)_{k,k}}{\partial x}\left(\tilde{\mathbf{K}}_{\mathbf{J}_{\mathrm{B}},\mathbf{J}_{\mathrm{B}}}\right)_{k,m}\frac{\partial\left(\tilde{\mathbf{G}}^{*}_{I_{\mathrm{C}},\mathrm{B}}\right)_{m,m}}{\partial x}\,\mathrm{d}x \tag{26}$$

$$\left(\mathbf{S}_{i_{\mathrm{E}},i_{\mathrm{C}},\mathrm{GR}}\right)_{k,m} = q^2A\int_{x_{p\mathrm{B}1}}^{w_{\mathrm{B}}-x_{p\mathrm{B}2}} \left(\tilde{\mathbf{G}}_{I_{\mathrm{E}},\mathrm{B}}\right)_{k,k}\left(\tilde{\mathbf{K}}_{\gamma_{\mathrm{B}},\gamma_{\mathrm{B}}}\right)_{k,m}\left(\tilde{\mathbf{G}}^{*}_{I_{\mathrm{C}},\mathrm{B}}\right)_{m,m}\,\mathrm{d}x. \tag{27}$$

Since the above integrals are amenable to analytic solution, they provide the pathway to a complete and accurate compact cyclostationary noise model for the bipolar transistor. The calculations are straightforward, albeit tedious, thus we will not show here for brevity the final formulae.

From the SCMs of the collector and emitter current (and their correlation), the statistical characterization of the base current noise can be easily derived starting from the condition $i_{\mathrm{B}} + i_{\mathrm{C}} + i_{\mathrm{E}} = 0$, valid also for the noisy signals.

This novel compact model has been preliminarily validated against 2-dimensional numerical PB drift-diffusion simulation results of a Si based npn BJT, with base length $W_{\mathrm{B}} = 150$ nm, $W_{\mathrm{E}} = 2\ \mu$m and $W_{\mathrm{C}} = 10\ \mu$m. The junction area is 5 mm^2. The doping levels are $N_{\mathrm{E}} = 10^{18}$ cm^{-3}, $N_{\mathrm{B}} = 5\times10^{17}$ cm^{-3} and $N_{\mathrm{C}} = 10^{16}$ cm^{-3}. The compact model, being valid for the intrinsic device, has been complemented by embedding the effect of the structure parasitics, namely the parasitic resistances $R_{\mathrm{E}} = 0.001\ \Omega$, $R_{\mathrm{B1}} = 0.4\ \Omega$ (extrinsic base), $R_{\mathrm{B2}} = 0.45\ \Omega$ (spreading base resistance), and $R_{\mathrm{C}} = 0.85\ \Omega$, including their thermal noise sources, and by the parasitic junction capacitances. The input tone is applied to the base-emitter voltage at a frequency of 1 MHz, and 4 harmonics have been included in the PB LS simulations.

We show in Fig. 7 (b) a comparison of the time-domain waveform for the collector current between the embedded compact model and the physics-based simulations, for several values of the time-varying input tone and a fixed $V_{\mathrm{CE}} = 3$ V. The agreement is always excellent. The same remark applies to the elements of the collector current SCM, shown in Fig. 7 (c).

DOI: 10.1002/jnm

Notice that to our knowledge this the first example of a complete and closed form LS model of the bipolar transistor including cyclostationary noise in a self-consistent way. In fact only approximate LS noise models based on MF or FM modulation schemes applied to stationary noise have been attempted so far. The availability of the accurate compact model can serve as a valuable simulation tool *per se* and also provide the reference against which the simplified models based on the MF or FM approach may be validated.

6. CONCLUSION

We have discussed the current status of cyclostationary noise modeling in high frequency active semiconductor devices, presenting in a unified manner the derivation of physics-based and compact device models. While in the physics-based case, at least for the more commonly employed PDE-based carrier transport description, the modeling roadmap is well traced (although many issues are still open, such as the accurate identification of the microscopic noise sources and the numerical efficiency of the simulations), the derivation of compact models still is an open research area. This is partly motivated by the lack of an easily available experimental characterization of cyclostationary noise, and by the intrinsic complexity of the physics of fluctuations in LS operation.

Finally, we have shown results of the physics-based simulation of the noise performances of a GaAs-HEMT based resistive mixer and we have presented a novel compact cyclostationary noise model for bipolar transistors, preliminarily validated against Si BJT physics-based simulations.

ACKNOWLEDGEMENTS

The authors wish to thank prof. Francesco Bertazzi of Politecnico di Torino for providing the results of the resistive mixer PB simulation.

REFERENCES

1. Phillips J, Kundert K. Noise in mixers, oscillators, samplers, and logic: an introduction to cyclostationary noise. *Proceedings of the IEEE Custom Integrated Circuits Conference (CICC)*, 2000; 431–439, doi:10.1109/CICC.2000.852702. URL http://www.designers-guide.org/Theory/cyclo-paper.pdf.
2. Bonani F, Donati Guerrieri S, Ghione G, Pirola M. A TCAD approach to the physics-based modeling of frequency conversion and noise in semiconductor devices under large-signal forced operation. *IEEE Trans. El. Dev.* May 2001; **48**(5):966–977, doi:10.1109/16.918245.
3. Bonani F, Donati Guerrieri S, Ghione G. Physics-based simulation techniques for small- and large-signal device noise analysis in rf applications. *IEEE Trans. El. Dev.* Mar 2003; **50**(3):633–644, doi:10.1109/TED.2003.810477. Invited paper.
4. Rudolph M, Bonani F. Low-frequency noise in nonlinear systems. *IEEE Microw. Mag.* Feb 2009; **10**(1):84–92, doi:10.1109/MMM.2008.930678.
5. Bonani F, Ghione G. *Noise in semiconductor devices*. Springer-Verlag, 2001.
6. Limiti E, Ciccognani W, Colangeli S. *Characterization and Modelling of High-Frequency Active Devices oriented to High-Sensitivity Subsystem Design*, chap. 3 in "Microwave De-Embedding: From Theory to Applications". Academic Press, 2014; 97–150.
7. Demir A, Sangiovanni-Vincentelli A. *Analysis and Simulation of Noise in Nonlinear Electronic Circuits and Systems*. Kluwer Academic Publisher, 1998.
8. Bonani F, Donati Guerrieri S, Ghione G. Noise source modeling for cyclostationary noise analysis in large-signal device operation. *IEEE Trans. El. Dev.* Sept 2002; **49**(9):1640–1647, doi:10.1109/TED.2002.802638.
9. Demir A, Mehrotra A, Roychowdhury J. Phase noise in oscillators: A unifying theory and numerical methods for characterization. *IEEE Trans. Circuits Syst. I, Fundam. Theory Appl.* May 2000; **57**(5):655–674.
10. Demir A. Phase noise and timing jitter in oscillators with colored-noise sources. *IEEE Trans. Circuits Syst. I, Fundam. Theory Appl.* December 2002; **49**(12):1782–1791.
11. Traversa FL, Bonani F. Oscillator noise: a nonlinear perturbative theory including orbital fluctuations and phase-orbital correlation. *IEEE Trans. Circuits Syst. I, Regul. Pap.* October 2011; **58**(10):2485–2497, doi:10.1109/TCSI.2011.2123531.
12. Jacoboni C. *Theory of Electron Transport in Semiconductors: A Pathway From Elementary Physics to Nonequilibrium Green Functions*. Springer-Verlag, 2010, doi:10.1007/978-3-642-10586-9.
13. Jungemann C, Meinerzhagen B. *Hierarchical Device Simulation. The Monte-Carlo Perspective*. Springer-Verlag, 2003, doi:10.1007/978-3-7091-6086-2.

14. Pérez S, González T, Delage S, Obregon J. Microscopic analysis of generation-recombination noise in semiconductors under dc and time-varying electric fields. *J. App. Phys.* July 2000; **88**(2):800–807, doi:10.1063/1.373739.
15. Shiktorov P, Starikov E, Gružinskis V, Pérez S, González T, Reggiani L, Varani L, Vaissière J. Upconversion of intergroup hot-carrier noise in semiconductors operating under periodic large-signal conditions. *Fluctuation Noise Lett.* Mar 2003; **3**:L51–L61, doi:10.1142/S0219477503001087.
16. Shiktorov P, Starikov E, Gružinskis V, Pérez S, González T, Reggiani L, Varani L, Vaissière J. Upconversion of partition noise in semiconductors operating under periodic large-signal conditions. *Phys. Rev. B* 2003; **67**:165 201, doi:10.1103/PhysRevB.67.165201.
17. Pérez S, González T, Delage S, Obregon J. Monte Carlo analysis of the influence of dc conditions on the upconversion of generation-recombination noise in semiconductors. *Semicond. Sci. Tech.* 2001; **16**:L8–L11, doi:10.1088/0268-1242/16/2/102.
18. Jungemann C. A deterministic approach to RF noise in silicon devices based on the Langevin-Boltzmann equation. *IEEE Trans. El. Dev.* May 2007; **54**(5):1185–1192, doi:10.1109/TED.2007.893210.
19. Hong SM, Pham AT, Jungemann C. *Deterministic Solvers for the Boltzmann Transport Equation*. Springer-Verlag, 2011, doi:10.1007/978-3-7091-0778-2.
20. Shiktorov P, Starikov E, Gružinskis V, González T, Mateos J, Pardo D, Reggiani L, Varani L, Vaissière J. Langevin forces and generalized transfer fields for noise modeling in deep submicron devices. *IEEE Trans. El. Dev.* Oct 2000; **47**(10):1992–1998, doi:10.1109/16.870587.
21. Jungemann C, Neinhus B, Meinerzhagen B. Hierarchical 2-D DD and HD noise simulations of Si and SiGe devices. I. Theory. *IEEE Trans. El. Dev.* Jul 2002; **49**(7):1250–1257, doi:10.1109/TED.2002.1013283.
22. Shockley W, Copeland J, James R. The impedance field method of noise calculation in active semiconductor devices. *Quantum Theory of Atoms, Molecules, and the Solid-State*, Lowdin PO (ed.). Academic Press, 1966.
23. Bonani F, Ghione G, Pinto M, Smith R. An efficient approach to noise analysis through multidimensional physics-based models. *IEEE Trans. El. Dev.* Jan 1998; **45**(1):261–269, doi:10.1109/16.658840.
24. Bonani F, Ghione G, Donati Guerrieri S, Varani L, Reggiani L. A general framework for the noise analysis of semiconductor devices operating in nonlinear (large-signal quasi-periodic) conditions. *Proc. of the 14th Int. Conf. on Noise in Physical Systems and* $1/f$ *noise*, Claeys C, Simoen E (eds.), World Scientific: Leuven, Belgium, 1997; 144–147.
25. Danneville F, Dambrine G, Cappy A. Noise modelling in MESFET and HEMT mixers using a uniform noisy line model. *IEEE Trans. El. Dev.* Oct 1998; **45**(10):2207–2212, doi:10.1109/16.725255.
26. Cappy A, Danneville F, Dambrine G, Tamen B. Noise analysis in devices under nonlinear operation Jan 1999; **43**(1):21–26, doi:10.1016/S0038-1101(98)00261-5.
27. Sanchez J, Bosman G, Law M. Two-dimensional semiconductor device simulation of trap-assisted generation-recombination noise under periodic large-signal conditions and its use for developing cyclostationary circuit simulation models. *IEEE Trans. El. Dev.* May 2003; **50**(5):1353–1362, doi:10.1109/TED.2003.813448.
28. Hong SM, Park CH, Park YJ, Min H. Physics-based analysis and simulation of $1/f$ noise in MOSFETs under large-signal operation. *IEEE Trans. El. Dev.* May 2010; **57**(5):1110–1118, doi:10.1109/TED.2010.2043186.
29. Bonani F, Donati Guerrieri S, Ghione G. Compact conversion and cyclostationary noise modeling of pn-junction diodes in low-injection. part I. Model derivation. *IEEE Trans. El. Dev.* Mar 2004; **51**(3):467–476, doi:10.1109/TED.2003.821570.
30. Bonani F, Donati Guerrieri S, Ghione G. Compact conversion and cyclostationary noise modeling of pn-junction diodes in low-injection. part II. Discussion. *IEEE Trans. El. Dev.* Mar 2004; **51**(3):477–485, doi:10.1109/TED.2003.821706.
31. Roy A, Enz C. Analytical modeling of large-signal cyclo-stationary low-frequency noise with arbitrary periodic input. *IEEE Trans. El. Dev.* Sept 2007; **54**(9):2537–2545, doi:10.1109/TED.2007.903200.
32. Rizzoli V, Neri A. State of the art and present trends in nonlinear microwave CAD techniques. *IEEE Trans. Microw. Theory Tech.* Feb 1988; **36**(2):343–365, doi:10.1109/22.3524.
33. Rizzoli V, Mastri F, Masotti D. General noise analysis of nonlinear microwave circuits by the piecewise harmonic balance technique. *IEEE Trans. Microw. Theory Tech.* May 1994; **42**(5):807–819, doi:10.1109/22.293529.
34. Heinen S, Kunisch J, Wolff I. A unified framework for computer-aided noise analysis of linear and nonlinear microwave circuits. *IEEE Trans. Microw. Theory Tech.* Dec 1991; **39**(12):2170–2175, doi:10.1109/22.106560.
35. Demir A, Liu E, Sangiovanni-Vincentelli A. Time-domain non Monte Carlo noise simulation for nonlinear dynamic circuits with arbitrary excitations. *IEEE Trans. Computer-Aided Design Integr. Circuits Syst.* May 1996; **15**(5):493–505, doi:10.1109/43.506137.
36. Roychowdhury J, Long D, Feldmann P. Cyclostationary noise analysis of large RF circuits with multitone excitations. *IEEE J. Solid-State Circuits* March 1998; **33**(3):324–336, doi:10.1109/43.506137.
37. van Vliet K. General transport theory of noise in pn junction-like devices – I: Three-dimensional Greens function formulation 1972; **15**:1033–1053, doi:10.1016/0038-1101(72)90164-5.
38. Nallatamby JC, Prigent M, Camiade M, Sion A, Gourdon C, Obregon J. An advanced low-frequency noise model of GaInP/GaAs HBT for accurate prediction of phase noise in oscillators. *IEEE Trans. Microw. Theory Tech.* May 2005; **53**(5):1601–1612, doi:10.1109/TMTT.2005.847050.
39. Rudolph M, Lenk F, Llopis O, Heinrich W. On the simulation of low-frequency noise upconversion in InGaP/GaAs HBTs. *IEEE Trans. Microw. Theory Tech.* 2006; **54**(7):2954–2961, doi:10.1109/TMTT.2006.877055.
40. Traverso P, Florian C, Borgarino M, Filicori F. An empirical bipolar device nonlinear noise modeling approach for large-signal microwave circuit analysis. *IEEE Trans. Microw. Theory Tech.* Dec 2006; **54**(12):4341–4352, doi:10.1109/TMTT.2006.885991.
41. Bertazzi F, Bonani F, G C, Donati Guerrieri S, Ghione G. Physics-based mixer noise simulation. *Proc. of the international workshop on Integrated Nonlinear Microwave and Millimetre-wave Circuits*, Aveiro, Portugal, 2006; 102–105.